

EVALUATION OF RADIATIONS SCATTERED FROM WATWR PHANTOM USING EGS CODE

T. Akita, T. Tamiya, K. Tabushi and S. Koyama

*Department of Radiological Technology, Nagoya University School of Health sciences
1-1-20 Daiko-Minami, Higashi-ku, Nagoya city, 461-0043, Japan
safe_akita@yahoo.co.jp*

Abstract

Spiritualists increased radiation exposure in interventional radiology. It is considered that the most important factor is sideward radiations scattered from a patient. Therefore, it is important to evaluate characteristics of sideward-scattered radiations. In this work, the spectra of sideward-scattered radiations at various field sizes and X-ray tube voltage were calculated using EGS Monte Carlo simulation. Furthermore, the average and the effective energy were calculated by these spectra. As a result, although field sizes were changed, these spectra did not change. Moreover, when the X-ray tube voltage increased, the average and the effective energy became higher too.

1. Introduction

One of the advance areas in radiology and high technology medicine has been the field of interventional radiology. Therefore, the radiation exposure of spiritualists should not be ignored. The most important factor is regarded as the radiation scattered from a patient. In such a case, to understand the characteristic of the radiation is necessary for radiation protection and very important. Moreover, the sideward radiations scattered from water phantom should be evaluated. However, it is difficult for us to detect the spectra of the sideward radiation scattered from a patient.

In this report, we made a study on the characteristic of lateral scatterings using EGS4 Monte Carlo simulation^{1,2)}

2. Materials and Method

Sideward radiations scattered from water phantoms were simulated based on the Monte Carlo method. The model for the calculation is shown in figure 1. The quadrangular water phantom was 30 cm by 30 cm and the depth 20cm. FSD (Focus-Surface Distance) was 100cm. Fan beams were emitted from an x-ray source. Incident X-ray spectra from the source were generated with x-ray tube voltages of 80, 100 and 120 kV. These spectra were calculated by Birch-Marshall formula³⁾. Radiation fields were $5 \times 5\text{cm}^2$, $10 \times 10\text{cm}^2$ and $20 \times 20\text{cm}^2$. The distance between the water phantom and the detector was 50cm. ECUT and PCUT used for all simulations of this study were 0.521 and 0.01 MeV, respectively. The average and the effective energy were calculated with spectra of sideward-scattered radiations.

3. Results

3.1 Comparison with incident X-rays

Figs.2, 3 and 4 show spectra of incident X-rays and sideward-scattered radiations at each X-ray tube voltage in $20\text{cm} \times 20\text{cm}$ field size. Each spectrum was normalized with maximum photon count except for characteristic X-rays. As compared with incident X-rays, sideward-scattered radiations decreased the relative count in regions of the high and the low energy.

Table shows the average energy of incident X-rays and that of sideward-scattered radiations at each X-ray tube voltage in $20\text{cm} \times 20\text{cm}$ field size. Although the average energy of sideward-scattered radiations at 80kV was higher than

that of incident X-rays, those at 100 and 120kV were lower.

Table shows the effective energy of incident X-rays and those of sideward-scattered radiations at various X-ray tube voltage in 20cm × 20cm field size. The effective energy of sideward-scattered radiations was higher than that of incident X-rays at each voltage.

3.2 Field size dependence

Figure 5 shows photon count spectra of sideward-scattered radiations at 120kV X-ray tube voltage in each field size. Each spectrum was normalized with the maximum photon count in 20cm × 20cm field size. Total photon count increased at larger field sizes.

Figure 6 shows spectra of sideward-scattered radiations at 120kV X-ray tube voltage in each field size. All spectra are same shape.

3.3 X-ray tube voltage dependence

Figure 7 shows spectra of sideward-scattered radiations at various X-ray tube voltage in 20cm × 20cm field size. As X-ray tube voltage increased, the energy with maximum photon increased too.

4. Discussion

4.1 Comparison with incident X-rays

The low energy photon is absorbed in water phantom. On the other hand, high energy photon decreased its energy by interaction with the water. Therefore, it is considered that spectra of sideward-scattered radiations are decreased in the high and the low energy regions. The average energy of sideward-scattered radiations at x-ray tube voltages of 80kV was higher than that of the incident x-ray, because low energy regions of these radiations more decreased. When x-ray tube voltage was 100 or 120kV, the average energy of sideward-scattered radiations was lower than that of incident x-rays. It is considered that these radiations more decreased in high energy region.

4.2 Field size dependence

It is found that a figure of spectra is changed by a field size. The energy of sideward-scattered radiations close to detector is high because of a little attenuation. However, that of sideward-scattered radiations far from detector is low because of less attenuation. These results are not changed by the field size. Therefore, it is necessary to study these problems more deeply in future.

4.3 X-ray tube voltage dependence

The incident X-rays increased by the rise of x-ray tube voltage. Therefore, it is considered that sideward-scattered radiations are also increased.

5. Conclusion

When field sizes were changed, the spectra were not changed. As X-ray tube voltages were increased, the average and the effective energy were increased too. We could evaluate properties of sideward radiations scattered from a patient using EGS Monte Carlo simulation.

References

- 1) W. R. Nelson, H. Hirayama and D. W. O. Rogers: The EGS4 code system. SLAC Report-265, (1985).
- 2) Y. Namito and H. Hirayama, "LSCAT: low-energy photon –scattering expansion for the EGS4 Code", KEK Internal 2000-4 (2000).
- 3) R. Birch and M. Marshall: Computation of Bremsstrahlung X-ray Spectra and Comparison with Spectra Measured

with a Ge(Li) Detector, Phys. Med. Biol. **24**, 505-517 (1979).

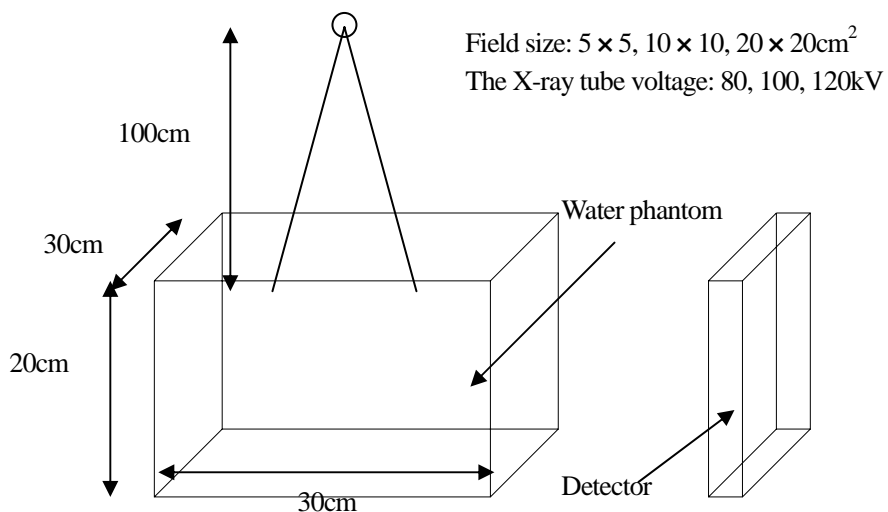


Fig.1 Geometrical conditions for simulation

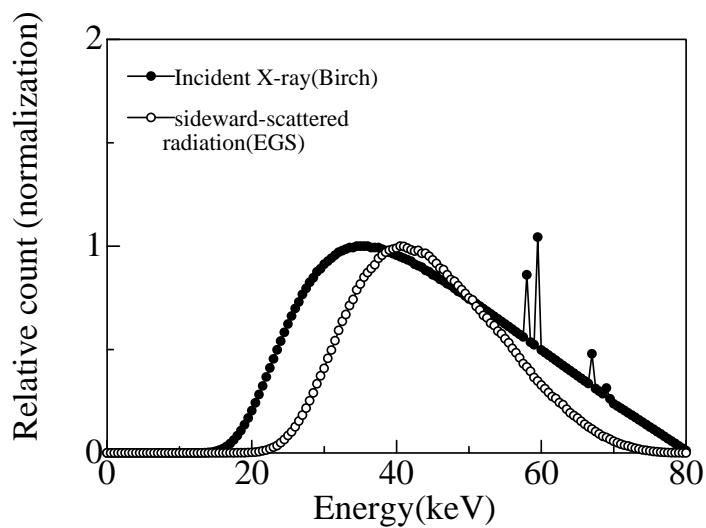


Fig. 2 Comparison between incident X-rays and sideward-scattered radiations (20cm x 20cm, 80kV)

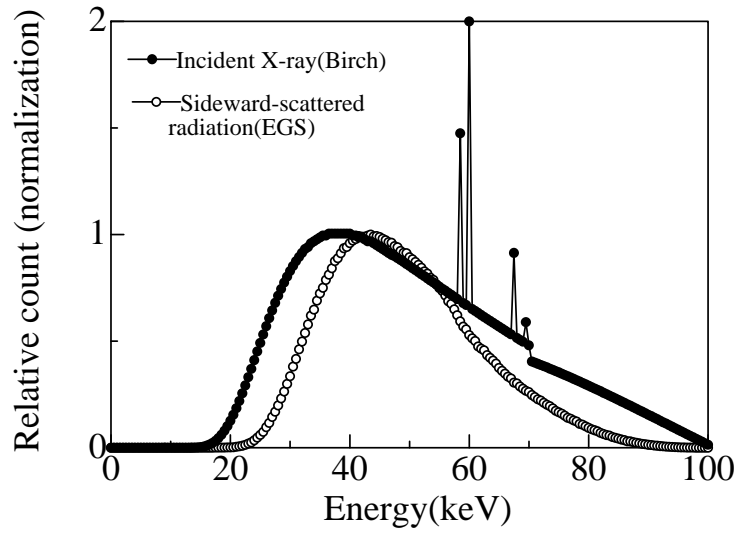


Fig. 3 Comparison between incident X-rays and sideward-scattered radiations (20cm × 20cm, 100kV)

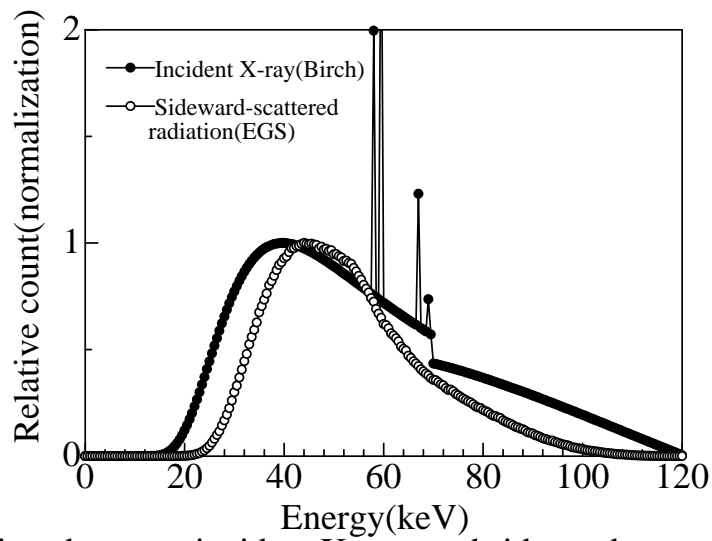


Fig. 4 Comparison between incident X-rays and sideward-scattered radiations (20cm × 20cm, 120kV)

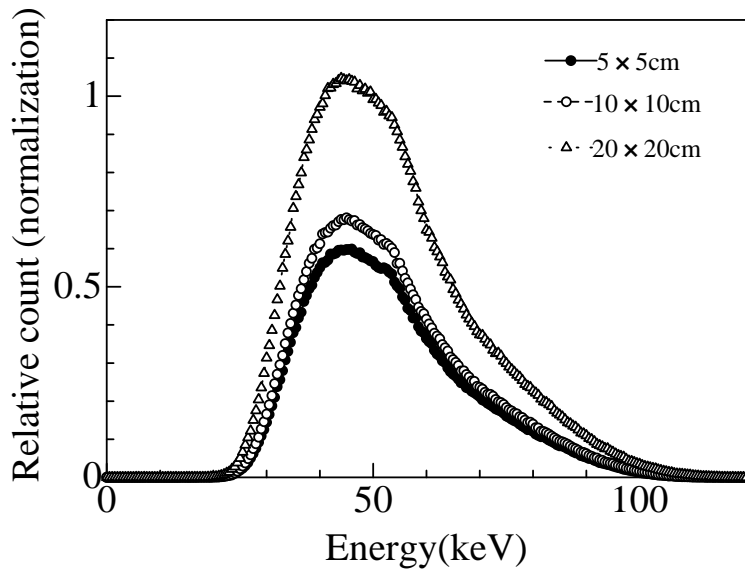


Fig. 5 Comparisons of relative photon count with different field sizes (120kV)

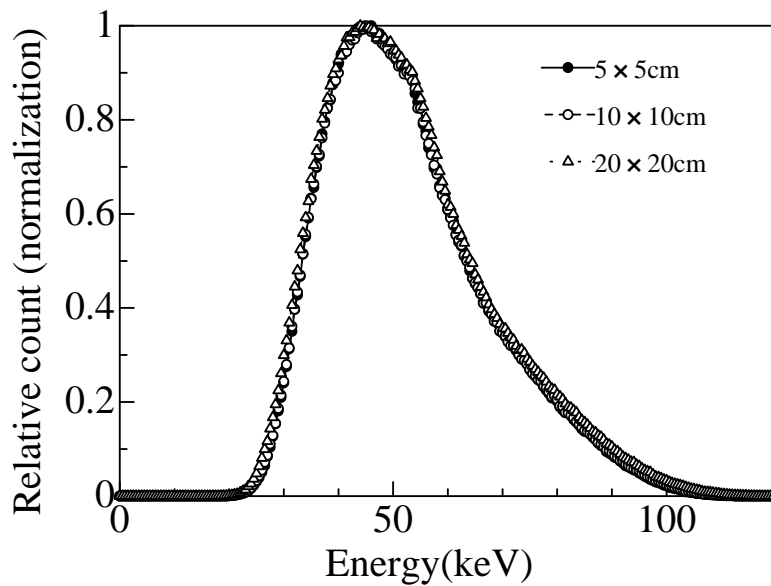


Fig. 6 Comparisons of sideward-scattered radiations spectra with different field sizes (120kV)

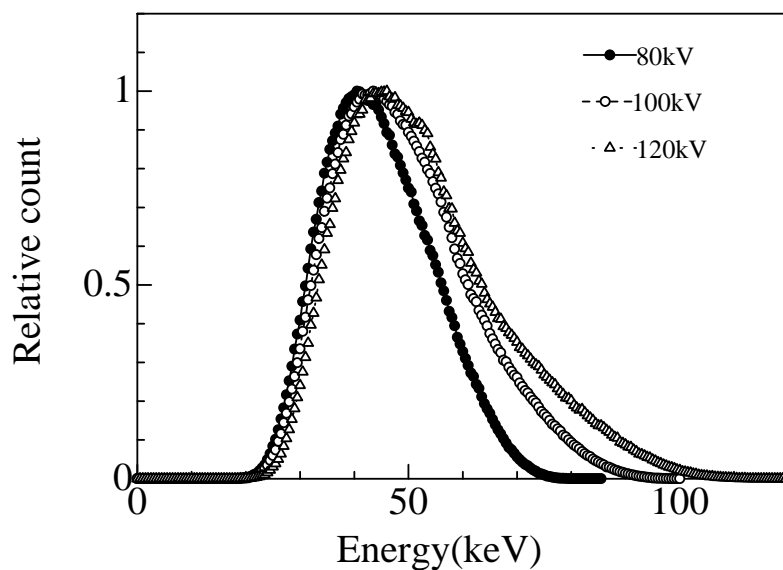


Fig. 7 Comparisons of sideward-scattered radiations spectra with different X-ray tube voltage (20cm × 20cm)

Table . Average energy with each condition

	X-ray tube voltage (kV)		
	80	100	120
Incident X-rays	43.7	50.5	55.6
Sideward-scattered radiations (5 × 5)	44.9	49.2	52.9
Sideward-scattered radiations (10 × 10)	44.9	49.2	53.0
Sideward-scattered radiations (20 × 20)	44.7	50.5	53.1

Table . Effective energy with each condition

	X-ray tube voltage (kV)		
	80	100	120
Incident X-rays	32.6	36.2	39.8
Sideward-scattered radiations (5 × 5)	38.3	40.9	43.5
Sideward-scattered radiations (10 × 10)	38.2	40.9	43.3
Sideward-scattered radiations (20 × 20)	37.5	40.4	42.8